NASA TECHNICAL MEMORANDUM

NASA TM X-71767

NASA TM X-71767

(NASA-TM-X-71767) EXPERIMENTALLY DETERMINED AEROACOUSTIC PERFORMANCE AND CONTROL OF SEVERAL SONIC INLETS (NASA) 22 p HC $3.25 CSCL 20D

N75-29353

Unclas

G3/34 31420

EXPERIMENTALLY DETERMINED AEROACOUSTIC PERFORMANCE AND CONTROL OF SEVERAL SONIC INLETS

by Brent A. Miller
Lewis Research Center
Cleveland, Ohio 44135

TECHNICAL PAPER to be presented at Eleventh Propulsion Conference cosponsored by the American Institute of Aeronautics and Astronautics and the Society of Automotive Engineers
Anaheim, California, September 29-October 1, 1975

E-8422

EXPERIMENTALLY DETERMINED AEROACOUSTIC PERFORMANCE AND CONTROL OF SEVERAL SONIC INLETS

Brent A. Miller*

National Aeronautics and Space Administration
Lewis Research Center
Cleveland, Ohio 44135

Abstract

Low speed wind tunnel tests were conducted to determine the aeroacoustic performance of several model sonic inlets. The results were analyzed to indicate how inlet aeroacoustic characteristics were affected by inlet design and operating conditions. A system for regulating sonic inlet noise reduction was developed and tested. Results indicate that pressure losses at forward velocity may be substantially less than those at static conditions. This is particularly true for translating centerbody inlets with the centerbody extended in the approach and landing position. Operation to simulated takeoff incidence angles of 50° was demonstrated with good inlet performance. Results suggest that at takeoff, with 0° incidence angle, sonic inlet total pressure losses need not exceed those generated by skin friction (e.g., without large diffusion or shock induced losses) for sound pressure level reductions to at least 15 dB. Inlet sound pressure level reduction was regulated to within approximately ±1 dB by controlling inlet surface static pressure measured at the diffuser exit. This system depends on a unique relationship between sound pressure level reduction and surface static pressure.

Introduction

Aircraft engine noise radiated forward through the inlet can be suppressed by accelerating the inlet flow to sonic or near-sonic velocity in the inlet throat(1-9). This high inflow velocity does not allow the forward propagating sound waves to escape from the inlet resulting in reduced engine noise. However, in order to successfully use this method of noise reduction, the inlet must be designed to achieve the necessary high inflow velocity with minimum aerodynamic penality. In addition, the basic operating characteristics of sonic inlets will impose severe constraints on engine operation leading to the possible requirement for variable engine or inlet geometry and an attendant control system.

This present paper presents the results of a wind tunnel investigation conducted to determine how the aeroacoustic performance characteristics of several sonic inlets were affected by inlet design and operating conditions. The data have been analized to indicate: (1) the effect of forward velocity and incidence angle on inlet aeroacoustic performance; (2) the level of total pressure loss that might be expected with well designed sonic inlet at takeoff where maximum engine thrust is required; and (3) how sonic inlet noise reduction can be regulated by measuring and controlling inlet surface static pressure. An evaluation of inlet mechanical design considerations, such as weight and complexity, is beyond the scope of this paper.

The effect of forward velocity on the relationship between total pressure recovery and sound pressure level reduction was investigated. This was done in order to judge the importance of testing at forward velocity when evaluating sonic inlet performance. In addition, the effect of operation at elevated incidence angles on total pressure recovery and total pressure distortion is presented as a function of sound pressure level reduction. The ability of the inlet to function well at incidence angles other than 0° is important. At takeoff and landing, where good aeroacoustic performance is required, the combined effects of engine location and wing upwash can produce large incidence angles between the inlet centerline and the local freestream velocity.

The noise reduction obtained with a fixed geometry sonic inlet was related to measurements of inlet surface static pressure and freestream total pressure. A control function was formed from these measurements that was used to regulate inlet noise reduction. No attempt was made to simulate engine dynamic characteristics. However, inlet flow was disturbed by increasing model incidence to the point of inlet flow separation. This was done in order to check the repeatability of the test results.

A possible automatic control method for a translating centerbody sonic inlet is described. The proposed control method makes use of a schedule relating noise reduction to centerbody position and measurements of inlet surface and freestream pressure. Although this automatic control system was not tested, tests were conducted with an adjustable position inlet to demonstrate the feasibility of generating the required control schedule.

The experimental results presented in this paper were obtained from tests of one fixed geometry and two translating centerbody type sonic inlets. The scale model inlets, with a diffuser exit diameter of 30.48 cm and design airflow of 11.68 kg/sec, were tested in the Lewis Research Center's 2.74 by 4.58-meter (9 x 15 foot) V/STOL wind tunnel(10). The tests were conducted without a fan or engine by using a vacuum system and the appropriate valves and controls to induce inlet airflow. A siren was used to simulate engine machinery noise so that the noise suppression properties of the inlets could be determined. Tests were conducted at static conditions and at a tunnel airflow velocity of 41 m/sec (80 knots). Data were obtained at incidence angles of 0° to 50°. Simultaneous measurements were made of the inlet total pressure recovery, total pressure distortion, and the reduction of siren tone sound pressure level.

*Aerospace Engineer, V/STOL and Noise Division.

Symbols

A_e	fan nozzle exit area
A_t	inlet minimum flow area (throat area)
A_1	diffuser exit flow area
D_{ct}	cowl throat diameter
D_e	diffuser exit diameter
D_h	hub diameter at diffuser exit
$D_{h\ell}$	inlet highlight diameter
D_m	inlet maximum outside diameter
$\mathcal{D}_{max}$	inlet total pressure distortion [(maximum total pressure) - (minimum total pressure)]/(average total pressure)
L_c	cowl length from highlight to diffuser exit
L_{cb}	centerbody length
M	flow Mach number
$\overline{M}_t$	average throat Mach number
N	engine speed, rpm
$N\sqrt{\theta}$	engine corrected speed, rpm
p	inlet surface static pressure
P_o	freestream total pressure
P_1	diffuser exit total pressure
P_2	fan exit total pressure
$\left(\frac{P_2}{P_1}\right)_{max}$	fan pressure ratio at maximum corrected flow
q_t	dynamic pressure at inlet throat
R	radius
R_t	inlet throat radius
S_w	internal wetted surface area
V_o	freestream velocity m/sec (knots)
W	weight flow, kg/sec
$\frac{W\sqrt{\theta}}{\delta}$	inlet corrected weight flow
$\left(\frac{W\sqrt{\theta}}{\delta}\right)^*$	inlet choking corrected weight flow
x	axial distance measured from highlight
y	centerbody position
Y	centerbody maximum travel
ΔP	difference between freestream total pressure and surface static pressure
$\Delta(SPL)_{BPF}$	reduction in one-third-octave band sound pressure level at siren blade passing frequency, dB
α	incidence angle (angle between local velocity or freestream velocity and inlet centerline), deg
β_{cb}	centerbody maximum wall angle, deg
β_d	diffuser maximum wall angle, deg
θ	inlet corrected temperature, (inlet air temperature in K)/(288.2 K)
δ	freestream corrected total pressure, P_o/101, 325 N/m^2

Discussion of Sonic Inlets

Sonic Inlet Basic Characteristics

The sketch at the top of figure 1 illustrates the operating principle of the sonic inlet. Engine noise suppression is achieved by accelerating the inlet flow to sonic or near sonic velocity in the inlet throat. This high inflow velocity does not allow the forward propagating sound waves to escape from the inlet. The flow velocity gradient generated within the inlet, indicated in the sketch by the arrows, bends the sound waves toward the wall. This refraction effect is thought to further suppress engine noise and has been investigated in reference 11.

Representative aeroacoustic behavior of a sonic inlet is illustrated in the lower half of figure 1. The figure indicates how sound pressure level reduction and total pressure recovery are typically affected by changing inlet airflow. Airflow is shown as a percent of choking or limiting airflow. A dual scale shows average throat Mach number computed assuming isentropic one-dimensional flow at the inlet throat.

The figure indicates that sound pressure level reduction and pressure recovery are strongly affected by small changes in inlet flow or average throat Mach number. Large sound pressure level reductions can be obtained by increasing the inlet flow toward the choking value, but with progressively poorer total pressure recovery. The rapid loss in recovery near choking flow occurs with the appearance of local shock boundary layer interactions within the inlet diffuser[12,13]. Well designed sonic inlets should operate to the left of this knee in order to obtain the maximum noise reduction with minimum aerodynamic penalty.

Performance Evaluation

In evaluating the aeroacoustic performance of a sonic inlet the trade between pressure recovery and noise reduction is of prime importance. High pressure recovery is required at takeoff for maximum thrust and at cruise for minimum fuel consumption. However, at approach and landing, pressure recovery may be secondary to maintaining an acceptable level of distortion with the desired noise reduction. Acceptable levels of distortion must, of course, be maintained at all conditions to minimize adverse effects on engine operation and the possible generation of additional noise.

Sonic inlet aeroacoustic performance can be readily evaluated by plotting inlet aerodynamic performance, for example, pressure recovery and distortion, as a function of the noise reduction obtained with the inlet. These data can be generated by operating the inlet over a relatively narrow range of weight flows near choking. A figure of this nature indicates how the requirement for various levels of noise reduction will effect inlet aerodynamic performance.

Effect of Sonic Inlet on Engine Operation

The significance of selecting a sonic inlet to reduce noise on engine operation can be illustrated with the aid of figure 2. This figure shows a typical turbine engine fan or compressor performance map relating pressure ratio and corrected weight flow. The vertical crosshatched flow limit line was obtained by assuming a fixed geometry sonic inlet sized to choke at 100 percent engine corrected airflow. Vertical lines showing constant values of sound pressure level reduction were then added using the data of figure 1.

Figure 2 indicates that a fixed geometry sonic inlet imposes two severe constraints on engine operation. First, in order to obtain a sizeable noise reduction, for example on the order of 20 dB, it is necessary to operate the inlet at approximately 97 percent of its choking airflow. If the inlet is sized to yield this noise reduction at aircraft takeoff, the engine maximum corrected airflow at all other flight conditions will effectively be limited to the takeoff value. The increase in corrected airflow often encountered during climb and cruise would be prevented by inlet choking. The inlet, by virtue of this potential flow limiting behavior, becomes a critical element in matching engine airflow and thrust to aircraft requirements.

The second constraint imposed by the inlet results from the rapid loss in noise suppression experienced with reduced engine airflow. This imposes a lower airflow limit below which the sonic inlet becomes ineffective as a noise suppressor. This becomes of consequence when noise suppression is desired at less than maximum engine thrust and airflow. This condition would normally arise during aircraft approach and landing.

These operating constraints imposed by a fixed geometry sonic inlet can be alleviated by restorting to variable geometry in the engine or inlet. For example, figure 3 indicates how a variable area nozzle could be used with a turbofan engine to maintain noise reduction at less than 100 percent engine thrust and airflow. A fixed geometry sonic inlet is assumed. The effect of increasing nozzle exit area on the relationship between engine thrust and airflow was computed at static conditions for a turbofan engine with a design fan pressure ratio of 1.5. The figure indicates that opening the exit nozzle will permit a high weight flow to be maintained while permitting the thrust to be reduced. For example if the approach thrust is assumed to be 70 percent of maximum thrust, a sound pressure level reduction at approach of 20 dB could be obtained by increasing the nozzle exit area to approximately 140 percent of its design value (point A). With the nozzle area fixed all noise suppression would be lost at 70 percent thrust (point B). However, nozzle area cannot be increased without limit. At some point flow problems resulting from separation or choking will occur in the stators or downstream duct limiting the effectiveness of this approach. For this reason, it is doubtful if this technique could be used to maintain noise suppression for conventional turbofan engines in most existing conventional takeoff and landing aircraft where the approach airflow is normally 65 to 75 percent of the takeoff value[14]. However, nozzle exit area variation could possibly be used successfully for short takeoff and landing aircraft where the approach thrust and airflow are somewhat higher.

If the sonic inlet is designed so that the throat area can be varied, noise reduction can be maintained with changing engine thrust and airflow. For constant noise reduction the required change in throat area is approximately equal to the change in engine corrected airflow. This change in inlet flow area allows the lines of constant noise reduction to be moved to the left in figure 3.

Sonic Inlet Types

Figure 4 shows a number of sonic inlet types that have been tested by a number of investigators. The simplest inlet is the fixed geometry type. However, as just described, this inlet will impose operating constraints on the engine. The other inlets shown have variable flow area obtained by translating a specially designed centerbody, contracting the cowl wall, or by retracting or translating vanes and rings within the inlet. Numerous variations of these basic inlet types, as well as several other inlet concepts, have also been proposed and in some cases tested[5,8]. In general, inlets containing vanes, rings, or other bodies immersed in the flow[8] have not performed as well as the other types shown in figure 4 and will not be discussed further in this paper.

Test Apparatus

Test Configurations

Data is presented in this paper for one fixed geometry and two translating centerbody sonic inlets. The translating centerbody inlets were tested with the centerbody retracted for takeoff and cruise and with it extended for approach and landing. The major geometric variables defining the design of the inlets are listed in Table I.

The fixed geometry inlet was designed with an overall length equal to the diffuser exit diameter. The diffuser area ratio of 1.21 yields a diffuser exit Mach number of 0.58 at choking airflow. The large internal lip contraction ratio was selected to obtain good inlet performance at high incidence angles. The diffuser contour is defined by a cubic equation with a slope parallel to the inlet centerline at the throat and diffuser exit. The maximum local wall angle of 8.7° occurs at the midpoint of the diffuser.

The two translating centerbody inlets differ primarily in diffuser (and therefore, overall) length. Both inlets have the same diffuser area ratio. With the centerbody retracted, the diffuser area ratio is 1.19 yielding a diffuser exit Mach number of 0.60 at choking airflow. With the centerbody extended the throat flow area is reduced 20 percent resulting in a diffuser area ratio of 1.47. At this condition the centerbody extends beyond the cowl. The maximum centerbody and diffuser wall angles are 10.2° and 10.7° respectively.

Facility

A schematic view of the test installation and facility is shown in figure 5. The tests were conducted in a 2.75- by 4.58-meter (9'x15') V/STOL wind tunnel. A vacuum system was used in place of a fan or compressor to induce inlet flow.

A venturi, calibrated in place against a standard ASME bellmouth that had been corrected for boundary-layer growth, was used to measure inlet airflow. The scatter in the airflow calibration data was approximately ±0.2 percent at the design inlet mass flow of 11.68 kg/sec (25.75 lbm/sec). Inlet airflow was remotely varied using two flow control valves arranged to give both course and find adjustment. Inlet incidence angle was also remotely varied by mounting the test apparatus on a turntable. A swivel joint, containing a low-leakage-pressure seal, provided 360° rotation capability.

Inlet total pressure recovery was computed at the simulated fan face using both hub and tip boundary layer rakes as well as total pressure rakes spanning the entire annulus. Eight full-span total pressure rakes were used with six equal-area-weighted tubes per rake. The hub and tip boundary-layer rakes each contained 5 total-pressure measurements. In computing total pressure distortion, $\mathcal{D}_{max}$, boundary-layer measurements taken closer to the wall than the nearest tube on the six-element equal-area-weighted rakes were omitted. This resulted in excluding those measurements closer to the wall than 8.3 percent of the annular area. The hub to tip ratio of the simulated fan face was 0.4.

To determine the acoustic suppression properties of the inlet using the vacuum flow system, a siren was installed in the duct downstream of the inlet. The siren was a 13.97-centimeter (5.5 in.) diameter single-stage fan with 16 blades modified by the addition of struts and a screen just upstream of the rotor to increase its noise level. The siren produced a fundamental blade passing tone at 8000 Hz. The siren was located approximately three inlet diameters downstream of the simulated fan face (fig. 5). Figure 5 also shows the microphones located in the wind tunnel approximately 20 meters upstream of the test section. The microphones were used to measure the siren noise transmitted through the inlet. The hardwalls of the wind tunnel approximate a reverberant chamber and eliminate any directional noise variation due to changing incidence angle.

The microphone outputs were recorded on magnetic tape and then processed with a one-third-octave band analyzer. The noise data presented in subsequent figures is for the one-third-octave band containing the 8000 Hz siren tone. These data are shown in terms of the noise reduction parameter $\Delta(SPL)_{BPF}$, where $\Delta(SPL)_{BPF}$ is the reduction in siren tone sound pressure level measured as the average throat Mach number is increased above 0.6. A correction of approximately 1.5 decibels was made in the siren source noise to account for convective flow effects within the duct as inlet weight flow was increased to the maximum value. A throat Mach number of 0.6 was selected to be representative of conventional inlets where no appreciable fan or compressor noise reduction due to throat Mach number is observed.

Performance

The effect of freestream velocity and incidence angle on sonic inlet aeroacoustic performance is presented in this section. Inlet aerodynamic performance is plotted versus sound pressure level reduction. As mentioned earlier, this method of data presentation indicates how the requirement for various levels of noise reduction will affect inlet aerodynamic performance.

Effect of Freestream Velocity

The change in inlet total pressure recovery due to freestream velocity is shown in figure 6. A comparison is made between the performance at static conditions and at a freestream velocity of 41 m/sec.

Figure 6(a) indicates that the pressure recovery measured with a fixed geometry (or takeoff configuration contracting cowl wall) inlet is substantially increased at freestream velocity compared to static conditions. The effect of freestream velocity is greatest at higher values of sound pressure level reduction where the inflow velocity is highest. This effect of freestream velocity results from the lower surface Mach numbers generated on the inlet surface at forward velocity[15].

Results obtained with the shorter translating centerbody inlet are shown in figure 6(b) with the centerbody in the retracted and extended positions. With the centerbody retracted in the takeoff and cruise position, static operation yielded a slightly lower pressure recovery than that measured at forward velocity for sound pressure level reductions below approximately 16 dB. At higher values of sound pressure level reduction, static operation resulted in a more rapid reduction in total pressure recovery. With the centerbody extended at static conditions, a rapid loss in pressure recovery was encountered at even the lowest values of sound pressure level reduction. This behavior resulted from flow separation within the diffuser. This diffuser separation was not present with forward velocity where the data for the centerbody retracted and extended positions show similar levels of total pressure recovery. Although not shown, similar results were also obtained with the longer translating centerbody inlet.

In summary, the results shown by figure 6 for these model tests indicate that static operation of a sonic inlet may yield pessimistic levels of total pressure recovery. This is particularly true for the translating centerbody inlet with the centerbody extended in the approach and landing position. Similar results might be expected with a contracting cowl wall inlet with the throat area contracted for approach and landing.

Effect of Incidence Angle

In general, sonic inlets will be forced to operate during takeoff and landing at incidence angles other than 0°. Figure 7 illustrates how the combined effects of engine location and wing upwash can produce large incidence angles between the engine centerline and the local velocity vector at the inlet entrance. In defining this angle the local velocity vector is assumed to be unaffected by the suction of the inlet. Under some operating conditions incidence angles of 40° to 50° could be encountered[16].

Figure 8 illustrates the effect of incidence angle on the radial Mach number distribution at the throat of a fixed geometry sonic inlet. These radial Mach number profiles were obtained from incompressible potential flow calculations corrected for compressibility[17]. The skewed profile obtained at 50° incidence angle results in an increased surface Mach number at the bottom of the inlet and a reduced Mach number at the top of the inlet. In addition to possibly generating flow problems on the inlet lip, the diffuser is presented with a more severely distorted flow than encountered at 0° incidence angle. Note also that although the average throat Mach number is 0.75, wide Mach number variations occur across the inlet throat. This might be expected to affect the acoustic performance of the inlet.

In order for a sonic inlet to operate successfully at high incidence angle, special care must be taken in designing the entry lip and diffuser in order to avoid flow separation. Theoretical analysis of inlet entry lips[15,18] indicates that tolerance to high incidence angle operation can be greatly improved by proper design. These references show that, with proper choice of inlet lip proportions and contraction ratio, the increase in surface Mach number and adverse pressure gradient encountered with increasing incidence angle (which may lead to flow separation) can be minimized.

Fixed Geometry Inlet - The aeroacoustic performance obtained with the fixed geometry inlet, which incorporated an inlet lip designed for high incidence angle operation, is shown in figure 9.

The model test results of figure 9 indicate that increasing incidence angle results in a loss in total pressure recovery and increased distortion for any given value of sound pressure level reduction. However, even at the severe 50° incidence angle condition at 41 m/sec freestream velocity, the general level of aeroacoustic performance is quite good. For example, at this condition, a sound pressure level reduction of 20 dB could be obtained with a total pressure recovery of 0.987 and a total pressure distortion of 10 percent. Additional detailed experimental and analytical results obtained with this inlet can be found in references 13 and 18.

Translating Centerbody Inlet - The effect of increasing incidence angle on the performance of the translating centerbody inlet with the long diffuser is shown in figure 10. With the centerbody retracted, figure 10(a) indicates a total pressure recovery of 0.982 at 50° incidence angle for a sound pressure level reduction of 20 dB. At this condition the total pressure distortion is approximately 12 percent. With the centerbody extended in the approach and landing position, figure 10(b), diffuser separation was encountered as incidence angle was increased beyond approximately 25°. This resulted in the increased total pressure loss and distortion shown at 30° incidence angle. Good aeroacoustic performance was obtained with the centerbody extended at incidence angles of 20° and below. Results presented in reference 9 suggest that improved performance might be obtained at high incidence angles by a slight retraction of the inlet centerbody with little decrease in the available throat area variation between the takeoff and approach positions.

Pressure Loss Correlation

Parameters relating total pressure loss to sound pressure level reduction were investigated for the three inlets in the takeoff configuration where minimum total pressure losses are desired. The data used were obtained at 0° and 30° incidence angle and 41 m/sec freestream velocity.

The first inlet total pressure loss coefficient investigated, defined as the loss in inlet total pressure divided by the throat dynamic pressure, is plotted in figure 11 versus sound pressure level reduction. This pressure loss coefficient should remain approximately constant with increased weight flow or noise reduction if the total pressure loss results from simple skin friction. The data at 0°, figure 11(a), and 30°, figure 11(b), incidence angle show this trend for the three inlets to a sound pressure level reduction of approximately 15 dB. At this point the longer translating centerbody inlet, with the higher loss coefficient, shows a rapid increase in pressure loss while the other inlets show a much smaller increase. This increased loss results from increased boundary layer thickness at the diffuser exit. This increase in boundary layer thickness is believed to result from the appearance of local shock-boundary layer interactions and diffusion losses within the inlet. The likelihood of this occurring in inlets with a high average throat Mach number is discussed in references 12 and 13.

With the assumption that inlet total pressure loss at moderate levels of sound pressure level reduction results from only skin friction, it follows that the pressure loss coefficient for different inlets should be similar when adjust to account for differences in inlet wetted surface area. This adjusted pressure loss coefficient is shown in figure 12 for the three inlets at 0° and 30° incidence angle. Results at 0° incidence angle, figure 12(a), indicate good agreement in the adjusted loss coefficient for the three inlets over a wide range of sound pressure level reduction. This result indicates that the higher loss measured with the longer translating centerbody inlet, even at moderate level levels of sound pressure level reduction, can be attributed to its greater wetted surface area. However at higher values of sound pressure level reduction the rapid increase in pressure loss resulting from diffusion losses and shock boundary layer interactions is again clearly evident.

The data obtained at 30° incidence angle, figure 12(b), indicate that losses are incurred with all three inlets in excess of those generated by skin friction. Unlike the data obtained at 0° incidence angle, the data at 30° indicate a progressive increase in the loss coefficient with increasing sound pressure level reduction. This indicates that diffusion and shock induced losses may be present at even the lowest values of sound pressure level reduction.

An explanation for this behavior can be obtained by returning to figure 8. This figure indicated that, at constant average throat Mach number, increasing incidence angle will result in locally high surface Mach numbers compared to the 0° case. These local regions of high Mach number contribute to the generation of additional total pressure losses.

In summary figure 12(a) indicates that, at 0° incidence angle, well designed fixed-geometry (or contracting cowl) and translating centerbody sonic inlets at takeoff may yield noise reduction to at least 15 dB without experiencing total pressure losses above those expected from skin friction. This figure also indicates that similar trades may exist between noise reduction and pressure loss for inlets of different types, but with comparable internal wetted surface area.

Operation at elevated incidence angle, figure 12(b), results in increased pressure loss owing to the formation of local regions of high surface Mach number and the appearance of diffusion losses. A comparison of the adjusted pressure loss coefficient for different inlets could possibly be used to identify those inlets suffering excess pressure loss resulting from poor design, or from severe operating conditions.

Inlet Control

In order to effectively utilize a sonic inlet, some method must be provided to control or regulate the noise reduction. The need for a control system can be illustrated with the aid of figure 13. This figure shows sound pressure level reduction as a function of percent of inlet choking corrected flow. The data indicate that if a sound pressure level reduction on the order of 20 dB is desired, it is necessary to operate on the steep portion of the curve where a 1 percent uncertainty or error in corrected airflow or throat area will result in a variation in the sound pressure level reduction of approximately 6 dB. This large variation in noise suppression is unacceptable, which leads to the requirement for an accurate control of inlet specific corrected flow. The control system may only need to function to make small trim adjustments in flow or inlet throat area about nominal values determined by the engine thrust setting. The inlet control problem could be eased by operating the inlet toward hard choke to ensure obtaining the required noise reduction. However, as illustrated in figure 1, this would result in increased inlet pressure loss with reduced engine thrust.

Approaches

One of two basically different methods could possibly be used to regulate sonic inlet noise reduction. With the first method engine external noise would be measured directly, and adjustments made in engine airflow or inlet throat area to maintain a specified noise level. This system requires microphones on the airframe or nacelles positioned so as to detect the noise emanating from a particular inlet with minimum interference from adjacent engines and other potential noise sources. With the second method the desired level of external noise would be maintained by operating the engine and inlet according to a pre-determined schedule relating sonic inlet noise reduction to an aerodynamic parameter such as percent of inlet choking airflow. The discussion to follow describes an inlet control system using the latter approach.

Control Signal

An inlet control system relating noise suppression to percent of inlet choking airflow requires a measurement of both inlet or engine airflow and inlet throat area. For fixed geometry inlets, the throat area is obviously known and presented no problem. For variable geometry inlets, throat area could be determined as a function of inlet position. The more difficult measurement to make is engine weight flow.

As depicted schematically in figure 14, inlet corrected flow could be derived either from measurement of engine operating conditions or from measurements made within the inlet itself. With the inlet airflow determined, inlet throat area is then used to compute percent of inlet choking airflow. A schedule similar to figure 13 then yields the sound pressure level reduction obtained with the inlet. This, when combined with the engine noise characteristics, determines the resulting external noise level.

Derivation of inlet corrected flow from engine measurements may require the monitoring of several engine conditions. Several factors that affect engine airflow are listed at the top left of figure 14. Nozzle area and blade angle, either stator or rotor, have been listed to indicate that any engine variable geometry features must be accounted for. For some engines, corrected airflow could possibly be obtained from a measurement of just engine corrected speed.

Derivation of inlet corrected flow from measurements made within the inlet may be, in some instances, a simpler approach and was the method adopted here. With this method the inlet is made to function somewhat like a flow meter. Inlet corrected flow is related to measurements of inlet surface static pressure and freestream total pressure. The selection of the location for the static pressure measurements within the inlet is important and is considered in figure 15.

Figure 15 shows the ratio of surface static pressure to freestream total pressure as a function of axial position within a fixed geometry sonic inlet. The effect of freestream velocity and incidence angle are shown for two values of inlet corrected weight flow. In order to use surface static pressure to determine corrected weight flow it is necessary to make the static pressure measurements in a portion of the inlet unaffected by either freestream velocity or incidence angle. For this inlet, figure 15 indicates that these conditions are met if the static pressure is measured downstream of the 0.4 x/L_c position. In this portion of the inlet, a measurement of surface static pressure can be used as a control signal to regulate inlet airflow, and hence sound pressure level reduction.

With this control technique it is possible to directly relate sound pressure level reduction to measurements of inlet static pressure without the intermediate step of computing corrected weight flow. This was done for the data of figure 13 and the result is shown in figure 16. For ease of measurement it is convenient to express the static pressure in terms of the simple inlet control function $\Delta P/P_o$, where:

$$\frac{\Delta P}{P_o} = \frac{P_o - P}{P_o} = 1 - \frac{P}{P_o}$$

The inlet static pressure was measured near the diffuser exit (x/L_c = 0.92, see fig. 15). Unlike corrected weight flow (plotted in fig. 13) this static pressure control function will continue to increase even for large values of sound pressure level reduction where inlet choking is approached. As defined, the control function is obviously not related to inlet flow when choking or large losses in total pressure occur within the inlet. It can more accurately be though of as measurement of the suction force applied to the inlet by the engine. In this light it is simply a convenient measurement that can be correlated against the sound pressure level reduction generated by any particular inlet. The relationship of the level of the control function to noise reduction will differ from inlet to inlet depending upon inlet design, and the location of the static pressure measurement. Nevertheless, a unique schedule should exist for each inlet. The next section describes how measurement and control of this static pressure was used to regulate the sound pressure level reduction of a fixed throat area sonic inlet.

Fixed Area Inlet - Figure 17 shows a schematic of the control system tested with a fixed geometry sonic inlet. The measurement of the inlet control function, $\Delta P/P_o$, was accomplished using the differential pressure transducer A and the absolute pressure transducer B. Surface static pressure was measured at the diffuser exit. The control function was obtained by dividing the transducer outputs. Note that with this measurement system, no obstructions are placed within the inlet airstream upstream of the engine.

As indicated in figure 17, the measured control function was compared to a pre-determined value selected to give a specified sound pressure level reduction. The difference between the two levels was nulled by adjusting inlet airflow. For the test rig this was accomplished with a throttle valve in the duct downstream of the inlet. With an engine this flow command could be used to make small adjustments in engine speed, nozzle area, or possibly some other variable affecting engine weight flow. The desired engine thrust and acceptable operating limits would of course have to be maintained.

Results obtained with this control system are shown in figure 18. Sound pressure level reduction and inlet total pressure recovery are shown as a function of incidence angle at a freestream velocity of 41 m/sec. The acoustic results, figure 18(a), indicate that a desired level of sound pressure level reduction could be maintained to within approximately ± 1 dB as incidence angle was increased from 0° to 50°. In order to check the repeatability of the results, the inlet flow was disturbed between the 0° incidence angle data points and all higher angle points by increasing the incidence angle to an excess of 70° resulting in entry lip and diffuser flow separation. The incidence angl was then reduced so that reattachment occurred. Data were then recorded at 25°, 40°, and 50° incidence angle. This procedure indicated that specific values of sound pressure level reduction could be repeated to within approximately ± 1 dB. Figure 18(b) indicates the drop in total pressure recovery that resulted from maintaining a constant sound pressure level reduction with increased incidence angle.

Variable Area Inlet - A possible control system for a translating centerbody sonic inlet is shown in figure 19. Inlet static pressure is measured in the manner previously described. Inlet airflow, and hence $\Delta P/P_o$, would be dictated by the engine thrust setting. The centerbody position would then be adjusted to yield the desired sound pressure level reduction according to a predetermined schedule. The required schedule relates centerbody position, y/Y, inlet static and freestream total pressure, $\Delta P/P_o$, and sound pressure level reduction. Although this control system has yet to be tested in the automatic mode tests have been conducted with an adjustable position centerbody inlet in order to determine the feasibility of developing the required control schedule. Some results of these tests are presented in figures 20 and 21.

Figure 20(a) shows sound pressure level reduction as a function of inlet corrected flow for several positions of the centerbody. Figure 20(b) shows the resulting variation of the control function, $\Delta P/P_o$, with sound pressure level reduction and centerbody position. These data were crossplotted to yield the control schedule shown in figure 21. This figure indicates the centerbody position required to maintain a specified sound pressure level reduction as the measured control function varies with engine airflow. At lower weight flows, where the centerbody is extended, the curves become steeper and somewhat closer together. In this region the inlet will be most sensitive to small changes in centerbody position or weight flow. This control schedule was generated at static conditions and the effects of forward velocity and incidence angle are not known. However, the figure does indicate that a schedule can be generated for use in the type of control system described in figure 19.

Summary of Results

Low speed wind tunnel tests were conducted with several scale model sonic inlets. The results were analyzed to indicate how the aeroacoustic characteristics of the inlets were affected by inlet design and operating conditions. A system for regulating sonic inlet noise reduction was developed and tested. The major results of this investigation may be summarized as follows:

1. Static tests of a sonic inlet may yield pessimistic levels of total pressure loss compared to the forward velocity case. This is particularly true for the translating centerbody inlet with the centerbody extended in the approach and landing position. Similar results might be expected with a contracting cowl wall inlet with the throat area fully contracted.

2. Although operating at forward velocity and high incidence angles skews the Mach number distribution at the inlet throat, sonic inlets can be designed to perform well at these conditions. A fixed geometry inlet demonstrated a total pressure recovery of 0.987 with total pressure distortion of 10 percent when operated at 50° incidence angle and 41 m/sec freestream velocity. At these conditions the sound pressure level reduction was 20 dB. With the same sound pressure level reduction and simulated flight conditions, a translating centerbody inlet in the takeoff configuration (centerbody retracted) yielded a total pressure recovery of 0.982 with a distortion of 12 percent. With the centerbody extended, diffuser separation was encountered at incidence angles greater than approximately 25°. However, good aeroacoustic performance was obtained at incidence angles of 20° and below.

3. The total pressure loss suffered by well-designed low diffuser area ratio sonic inlets in the takeoff configuration, at 0° incidence angle, may not exceed the level generated by simple skin friction (e.g., without large diffusion or shock induced losses) for sound pressure level reductions to at least 15 dB. At higher levels of noise suppression, or at elevated incidence angles, diffusion losses and local shock-boundary layer interactions may be encountered with a rapid increase in pressure loss.

4. With the assumption that inlet total pressure loss resulted solely from skin friction, a loss coefficient was defined adjusted to account for inlet wetted area. For moderate levels of sound pressure level reduction, at 0° incidence angle, this adjusted loss coefficient was shown to be similar for the fixed geometry (or contracting cowl wall) and translating centerbody inlets at takeoff. The appearance of local shock-boundary-layer interactions and diffusion losses were readily evident by a rapid increase in this loss coefficient. Comparison of this adjusted loss coefficient for different inlet types could possibly be used to identify inlets suffering excess pressure loss resulting from poor design or from severe operating conditions.

5. The use of a sonic inlet to suppress noise requires a control system capable of regulating inlet throat specific flow with less than 1 percent deviation in order to obtain sound pressure level reductions on the order of 20 dB with minimum aerodynamic loss. A control system capable of this accuracy was tested with a fixed geometry inlet by generating a schedule relating sound pressure level reduction to a measurement of inlet surface static pressure and freestream total pressure. A control function was formed from these pressure measurements that could be used to regulate sound pressure level reduction with approximately ± 1 dB variation.

6. A possible automatic control method for a translating centerbody sonic inlet was described. The proposed control method makes use of a schedule relating sound pressure level reduction to centerbody position and measurements of inlet surface and freestream pressure. Although the automatic control system was not tested, tests were conducted with an adjustable position centerbody inlet. The results of these tests indicate that the required control schedule can be generated.

Concluding Remarks

The results presented in this paper indicate that sonic inlets can be designed to reduce inlet emitted engine noise without excessive losses in inlet total pressure. This result is generally true even when operating at the severe conditions imposed by high incidence angles. Any difference in performance at takeoff between well designed sonic inlets of the types discussed in this paper may, for low values of incidence angle, simply result from differences in inlet internal wetted surface area. The selection of a particular type of sonic inlet may well depend more upon mechanical design considerations then the relationship between pressure loss and noise suppression. This may be especially true for variable-area inlets where the ease of accomplishing the geometry change will be an important consideration.

An area of special concern with sonic inlets relates to maintaining the desired level of noise reduction without experiencing unnecessary total pressure and thrust losses. The need for a control system capable of accurately regulating inlet throat specific flow is clearly indicated. The control approach investigated in this paper appears attractive. However, these results were obtained under laboratory test conditions and further analysis and experimentation is required to access the methods application to operational engine use. Some information of this nature will be forthcoming from the Lewis Quiet-Clean Short-Haul Experimental Engine program. The low pressure ratio turbofan engine to be developed in this program features a fixed area high throat Mach number inlet along with a variable area fan nozzle and variable pitch fan. Measurements of inlet surface static pressure will be used to make trim adjustments in nozzle exit area in order to maintain the desired level of inlet radiated noise.

Control of sonic inlet operation by direct measurement of external noise may be feasible and warrants investigation. This approach may offer the advantage of eliminating the need for a predetermined control schedule with a measurement of external noise used to make trim adjustments in inlet or engine operation. Regardless of the control method ultimately selected, it must not impare safe operation of the engine during both normal and emergency conditions (e.g., with control system component failure) while yielding the desired acoustic performance.

References

1. Chestnutt, D., "Noise Reduction by Means of Inlet-Guide-Vane Choking in an Axial-Flow Compressor," TN D-4682, July 1968, NASA.
2. Miller, B. A. and Abbott, J. M., "Aerodynamic and Acoustic Performance of Two Choked Flow Inlets Under Static Condition," TM X-2629, Sept. 1972, NASA.
3. Miller, B. A. and Abbott, J. M., "Low-Speed Wind Wind-Tunnel Investigation of the Aerodynamic and Acoustic Performance of a Translating-Centerbody Choked-Flow Inlet," TM X-2773, June 1973, NASA.
4. Klujber, F., "Results of an Experimental Program for the Development of Sonic Inlets for Turbofan Engines," AIAA Paper 73-222, Washington, D.C., Jan. 1973.
5. Klujber, J. C., Bosch, J. C., Demetrick, R. W. and Robb, W. L., "Investigation of Noise Suppression by Sonic Inlets for Turbofan Engines. Volume I: Program Summary," D6-40855, Jul. 1973, Boeing Commercial Airplane Co., Seattle, Wash., also NASA CR-121126.
6. Abbott, J. M., Miller, B. A., and Golladay, R. L., "Low-Speed Wind-Tunnel Investigation of the Aerodynamic and Acoustic Performance of a Translating-Grid Choked-Flow Inlet," TM X-2966, Feb. 1974, NASA.
7. Groth, H. W., "Sonic Inlet Noise Attenuation and Performance with a J-85 Turbojet Engine as a Noise Source," AIAA Paper 74-91, Washington, D.C., Jan. 1974.
8. Abbott, J. M., "Aeroacoustic Performance of Scale Model Sonic Inlets," AIAA Paper 75-202, Pasadena, Calif., Jan. 1975.
9. Hickcox, T. E., Lawrence, R. L., Syberg, J. and Wiley D. R., "Low Speed and Angle of Attack Effects on Sonic and Near-Sonic Inlets," D6-42392, Mar. 1975, Boeing Commercial Airplane Co., Seattle, Wash., also NASA CR-134778.
10. Yuska, J. A., Diedrich, J. H. and Clough, N., "Lewis 9- by 15-Foot V/STOL Wind Tunnel," TM X-2305, July 1971 NASA.

11. Sloan, D. and Farquahar, B. W., "The Refracting Inlet: A New Concept for Aircraft Inlet Noise Suppression," ASME Paper 75-GT-21, Houston, Texas, 1975.

12. Jakubowski, A. K. and Luidens, R. W., "Internal Cowl-Separation at High Incidence Angles," AIAA Paper 75-64, Pasadena, Calif., Jan. 1975.

13. Miller, B. A., Dastoli, B. J. and Wesoky, H. L., "Effect of Entry-Lip Design on Aerodynamics and Acoustics of High Throat-Mach-Number Inlets for the Quiet, Clean, Short-Haul Experimental Engine," TM X-3222, May 1975.

14. Hodge, C. G., Winslow, L. J., and Wood, S. K., "The Effect of Inlet-Noise Suppression on Propulsion System Design," AIAA Paper 73-1294, Las Vegas, Nev., Nov. 1973.

15. Albers, J. A. and Miller, B. A., "Effect of Subsonic Inlet Lip Geometry on Predicted Surface and Flow Mach Number Distributions," TN D-7446, Dec. 1973, NASA.

16. Albers, J. A., "Predicted Upwash Angles at Engine Inlets for STOL Aircraft," TM X-2593, Jul. 1972, NASA.

17. Albers, J. A. and Stockman, N. O., "Calculation Procedures for Potential and Viscous Flow Solutions for Engine Inlets," ASME Paper 74-GT-3, Mar. 1974.

18. Albers, J. A., Stockman, N. O., and Hirn, J. J., "Aerodynamic Analysis of Several High Throat Mach Number Inlets for the Quiet Clean Short-Haul Experimental Engine," TM X-3183, Jan. 197 1975, NASA.

E-8422

TABLE I. - INLET GEOMETRIC VARIABLES AND NOMENCLATURE

(a) Geometric variables

Geometric variable	Inlet type		
	Fixed geometry	Translating centerbody	
		Short diffuser	Long diffuser
	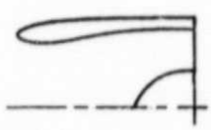		
Ratio of cowl length to diffuser exit diameter, L_c/D_e	1.0	0.79	1.0
Ratio of diffuser exit flow area to inlet throat area, A_1/A_t	1.21	1.49 1.19	1.49 1.19
Ratio of centerbody length to cowl length, L_{cb}/L_c	0.3	1.2 0.79	1.17 0.85
Internal lip contraction ratio, $(D_{h\ell}/D_{ct})^2$	1.46	1.38	1.38
External forebody diameter ratio, $D_{h\ell}/D_m$	0.905	0.86	0.86
Centerbody diameter ratio at diffuser exit, D_h/D_e	0.4	0.4	0.4
Ratio of diffuser exit area to internal wetted surface area, A_1/S_w	0.21	0.18 0.20	0.143 0.158
Maximum centerbody wall angle, β_{cb}, deg	-----	10.2	10.2
Maximum diffuser wall angle, β_d, deg	8.7	10.7	10.2

(b) Nomenclature

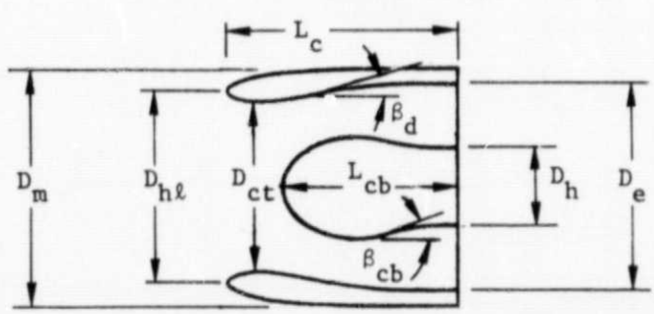

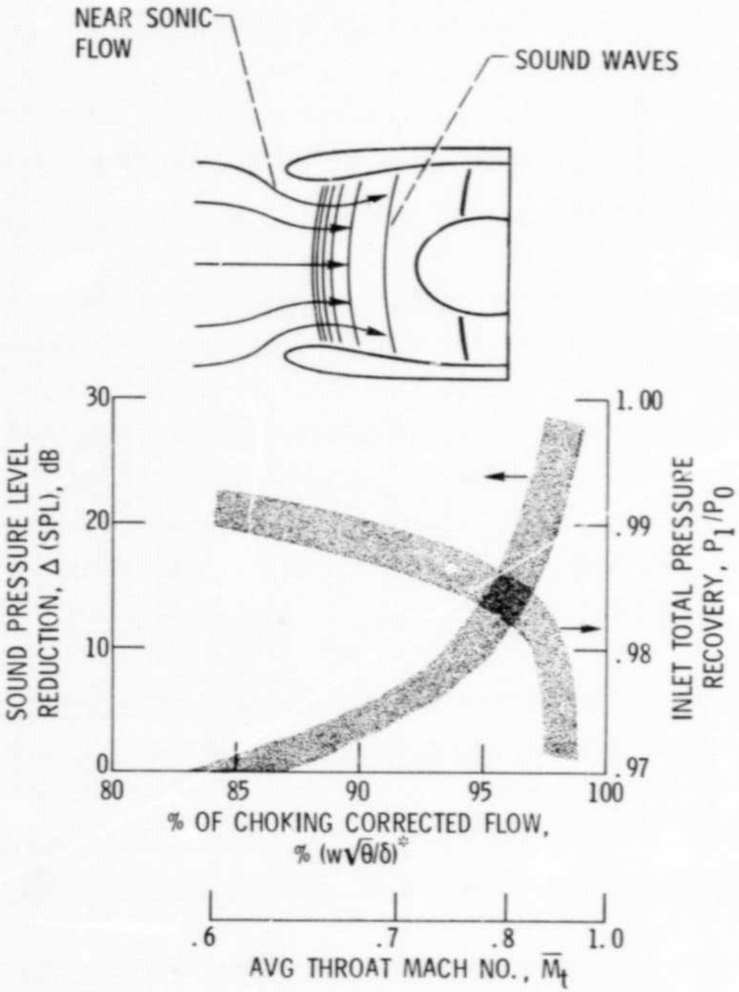

Figure 1. - Aeroacoustic performance typical of a fixed geometry sonic inlet.

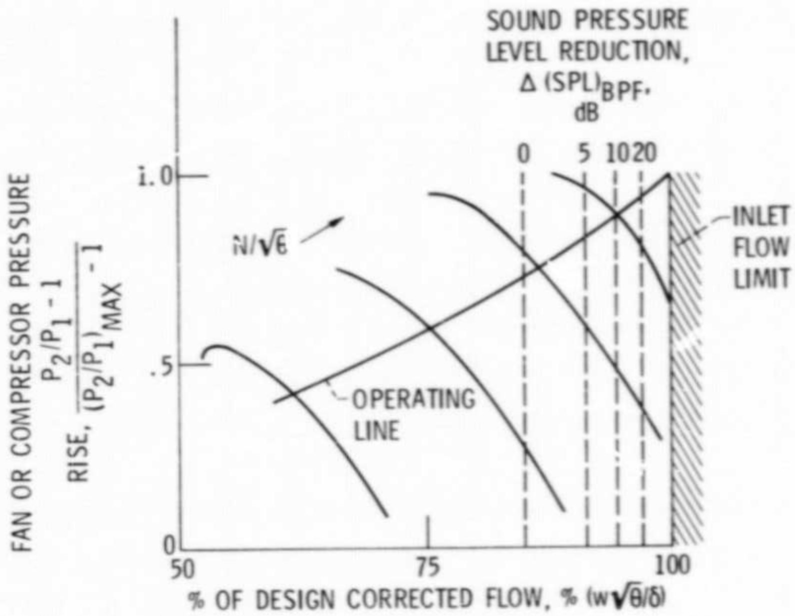

Figure 2. - Region on fan or compressor map where noise suppression can be obtained with a fixed geometry sonic inlet.

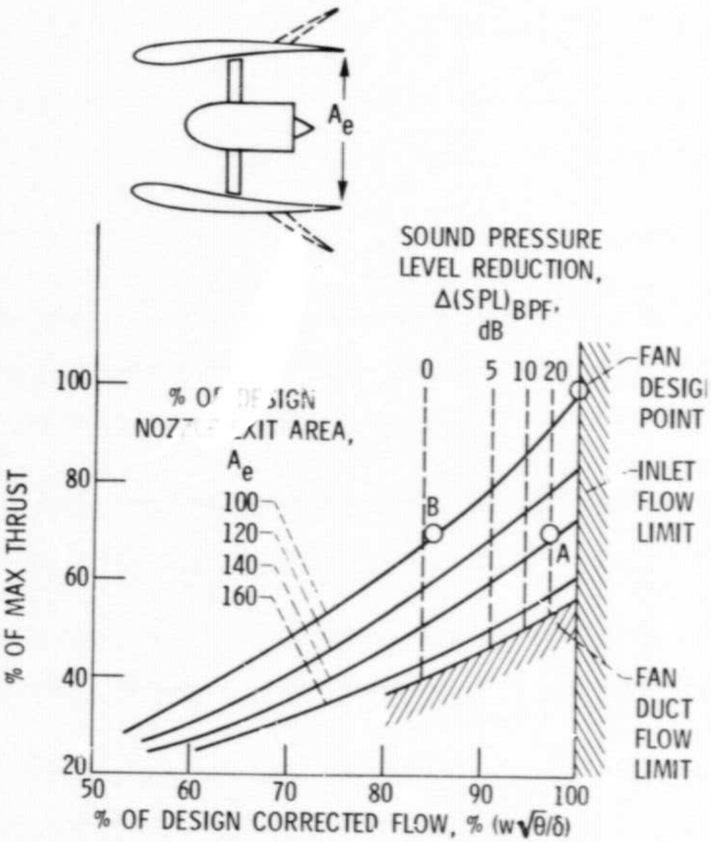

Figure 3. - Effect of increasing fan nozzle exit area on thrust and noise reduction. Results computed at static conditions with fan design point pressure ratio of 1.5.

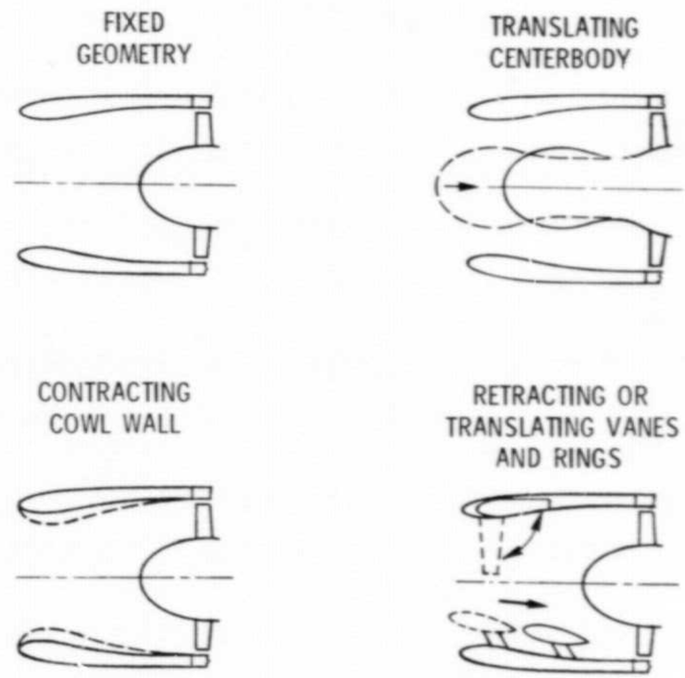

Figure 4. - Sonic inlet types.

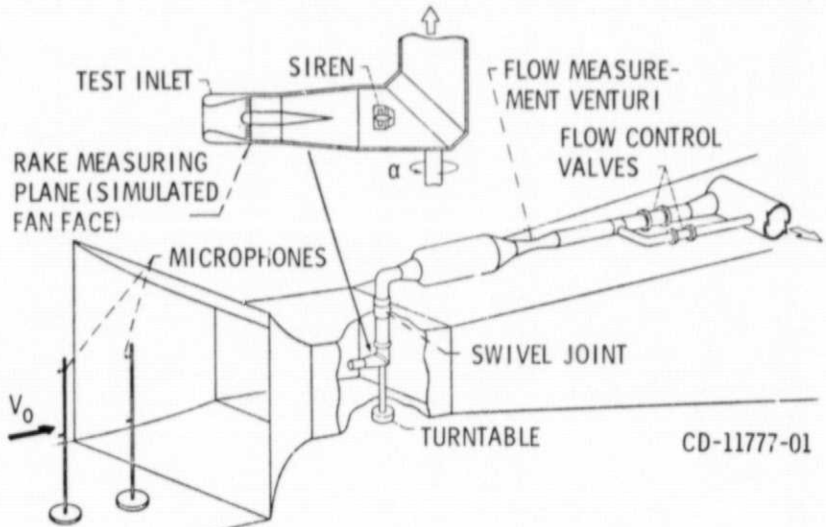

Figure 5. - V/STOL wind tunnel showing model arrangement and microphone locations.

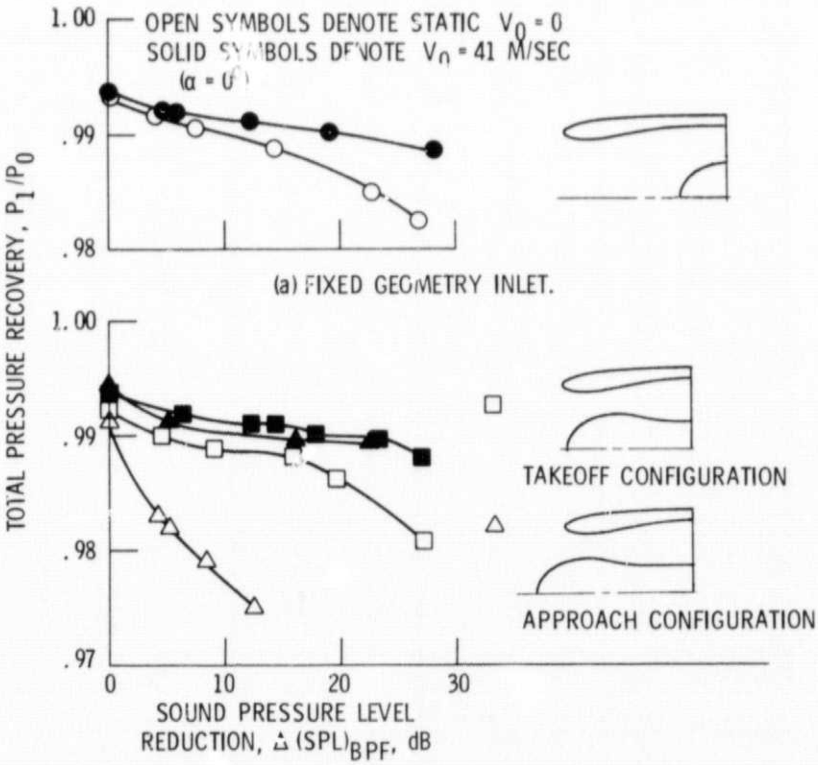

Figure 6. - Effect of free stream velocity on inlet performance.

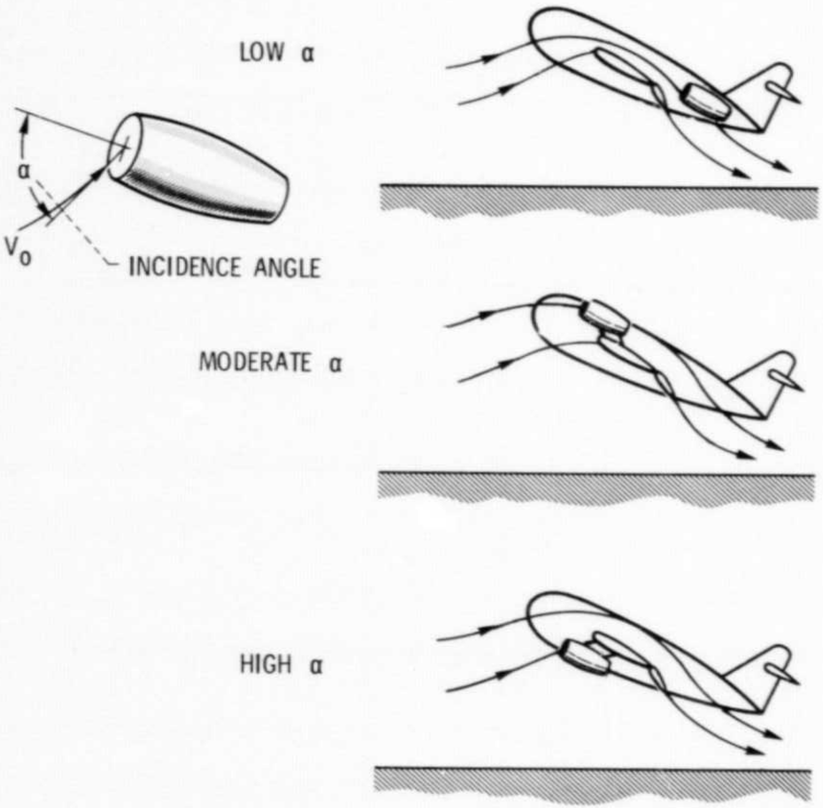

Figure 7. - Effect of engine location and wing upwash on inlet incidence angle.

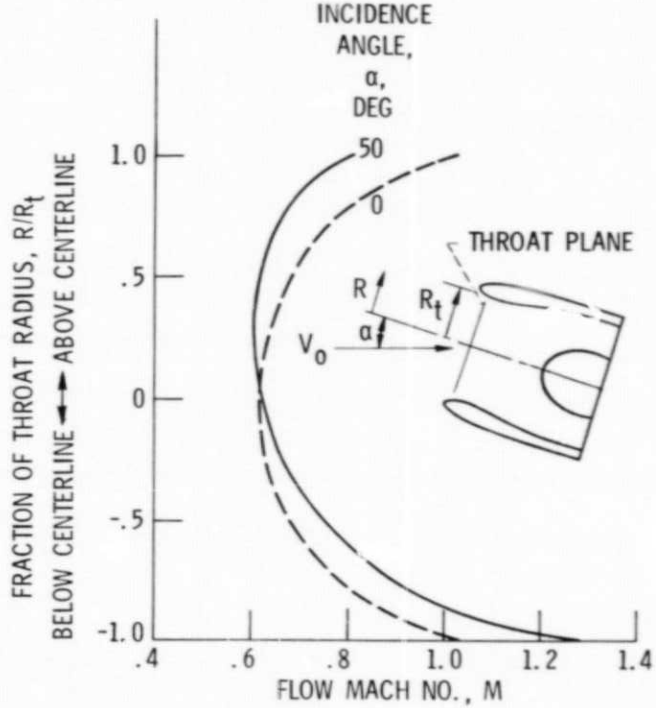

Figure 8. - Typical radial distribution of throat Mach number in a sonic inlet. Results of potential flow calculation; free stream velocity, V_o, 41 meters per second (80 knots); average throat Mach number, $\overline{M}_t$, 0.75.

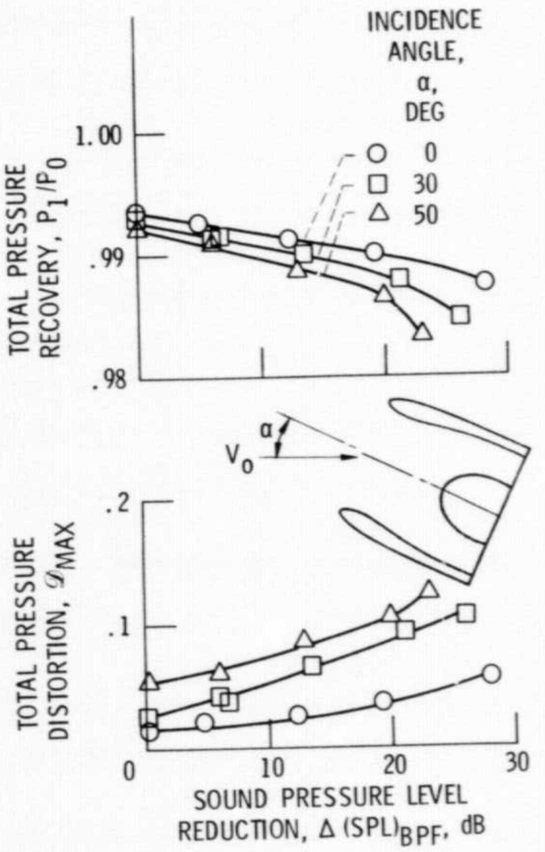

Figure 9. - Effect of incidence angle on acroacoustic performance of fixed geometry sonic inlet. Free stream velocity, V_0, 41 meters per second (80 knots).

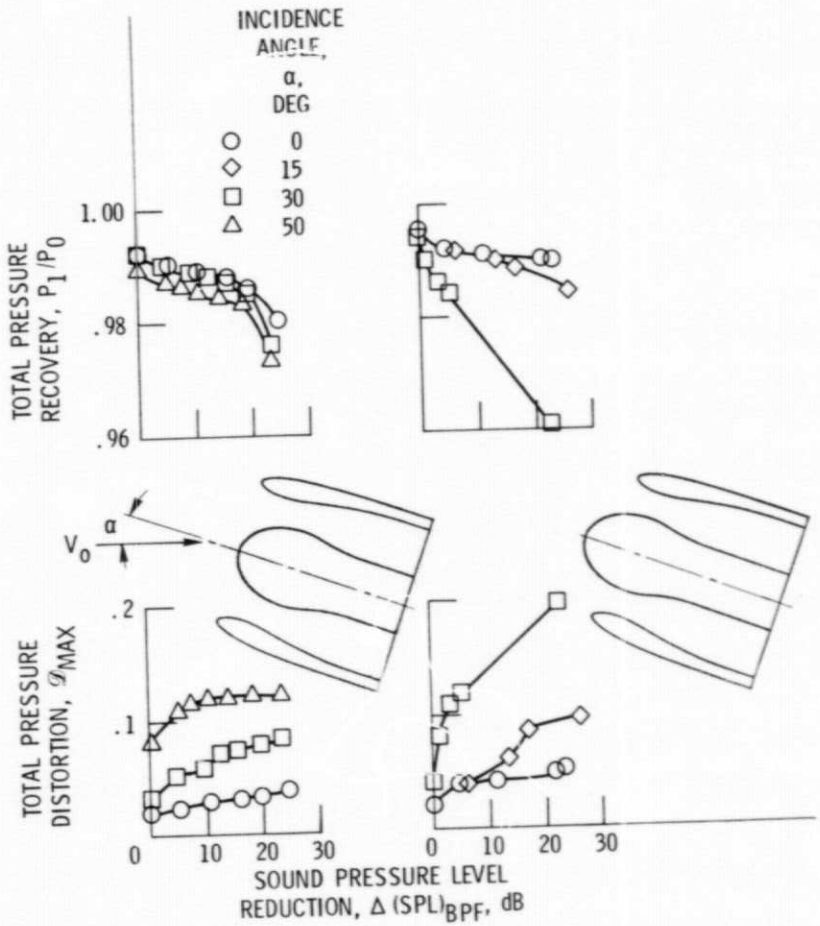

(a) CENTERBODY RETRACTED (TAKEOFF).

(b) CENTERBODY EXTENDED (APPROACH).

Figure 10. - Effect of incidence angle on aeroacoustic performance of translating centerbody inlet with long diffuser. Free stream velocity, V_0, 41 meters per second (80 knots).

E-8422

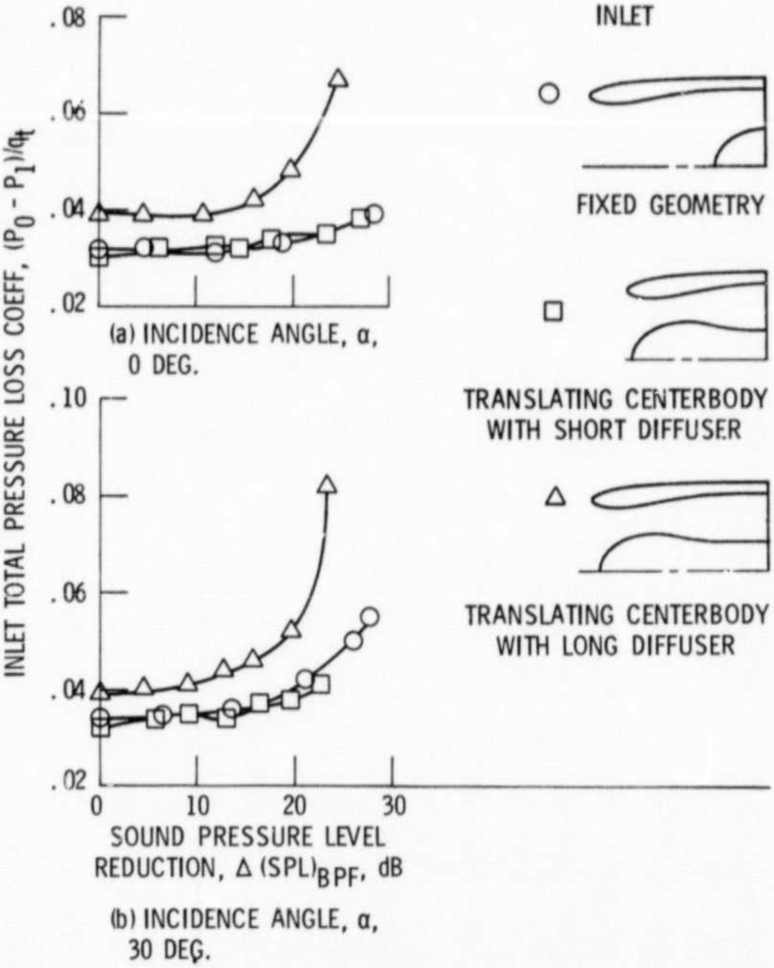

Figure 11. - Inlet total pressure loss coefficient as a function of sound pressure level reduction for several sonic inlets in the takeoff configuration. Free stream velocity, V_0, 41 meters per second (80 knots).

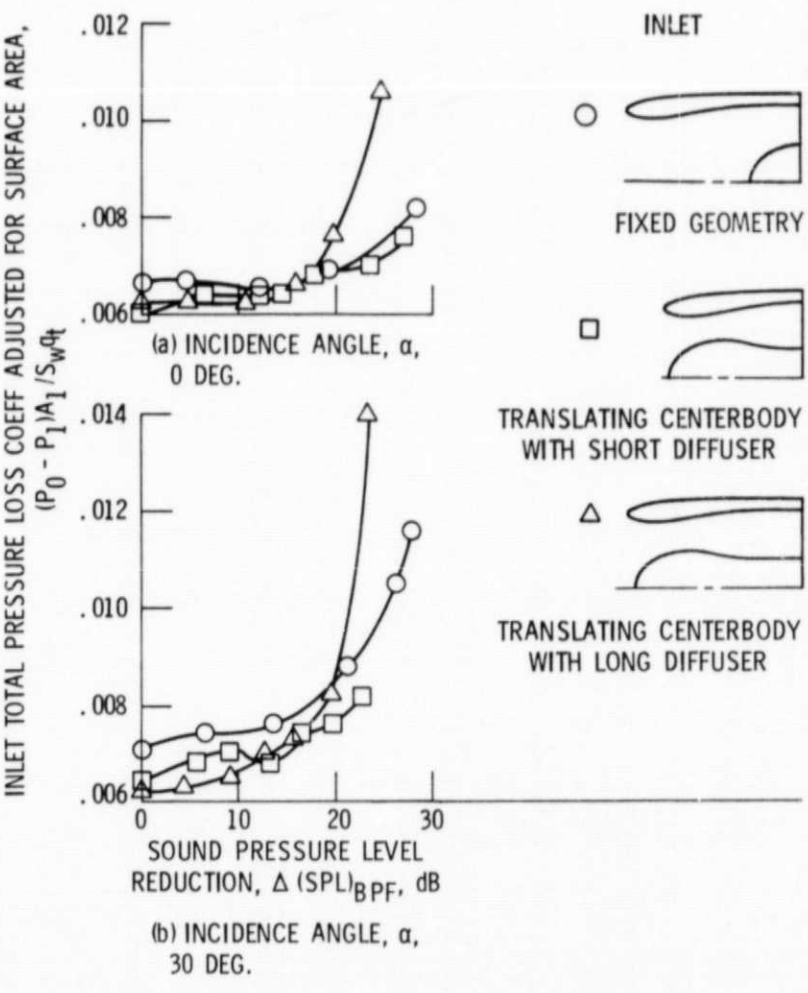

Figure 12. - Inlet total pressure loss coefficient adjusted for wetted surface area as a function of sound pressure level reduction for several sonic inlets in the takeoff configuration. Free stream velocity, V_0, 41 meters per second (80 knots).

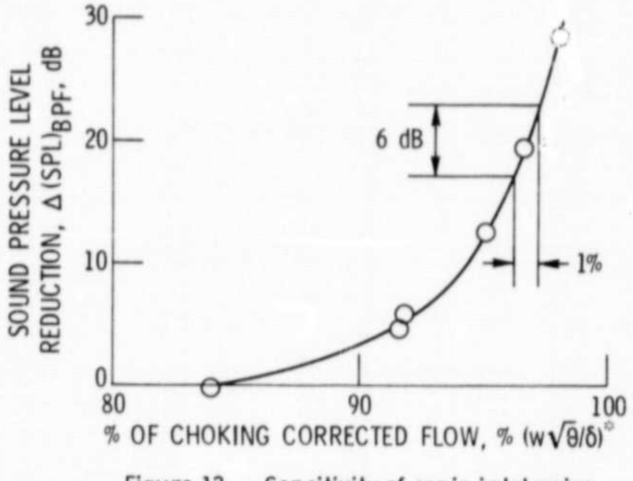

Figure 13. - Sensitivity of sonic inlet noise suppression to inlet flow.

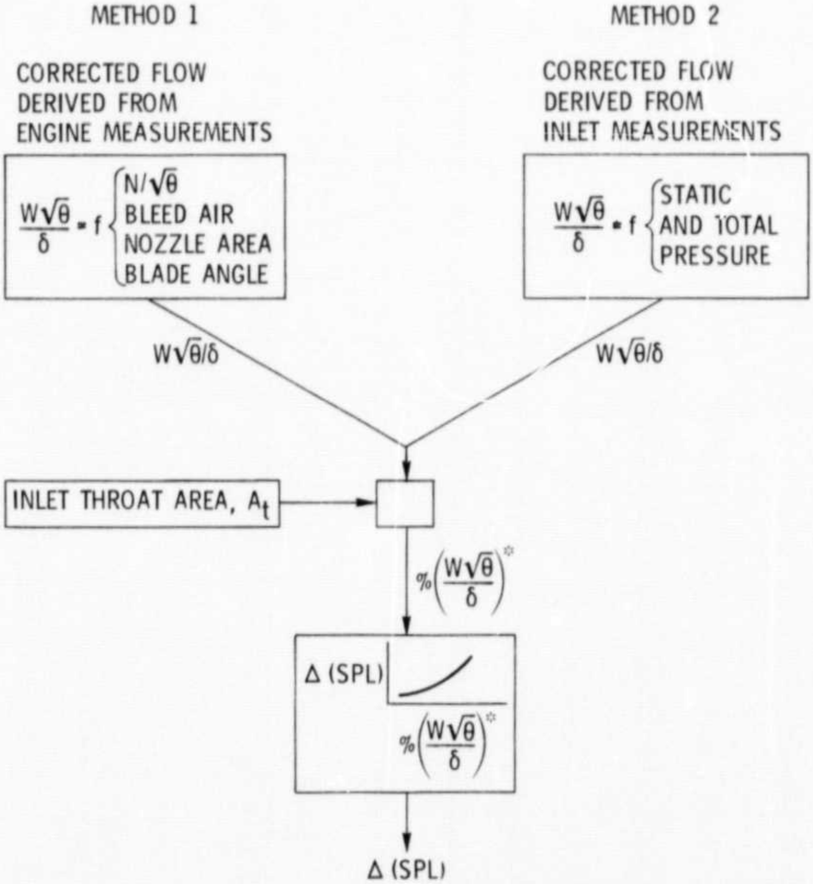

Figure 14. - Two possible methods for determining inlet corrected flow, and hence sonic inlet noise reduction.

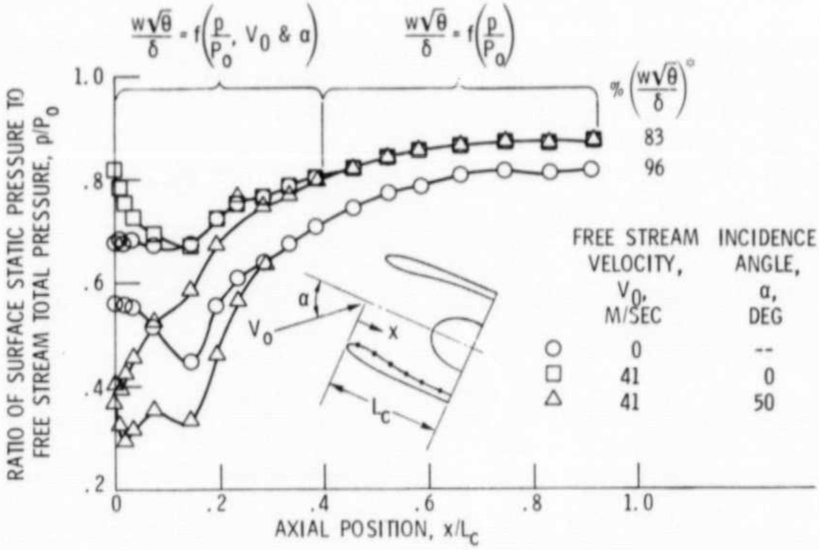

Figure 15. - Selection of inlet surface static pressure measurement to determine inlet weight flow.

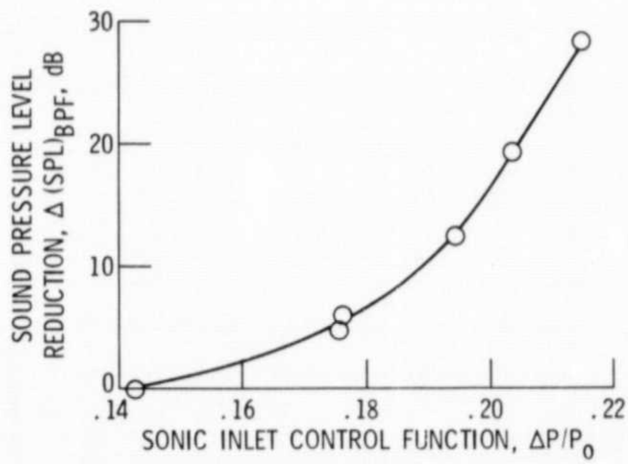

Figure 16. - Sensitivity of sonic inlet noise reduction to inlet control function.

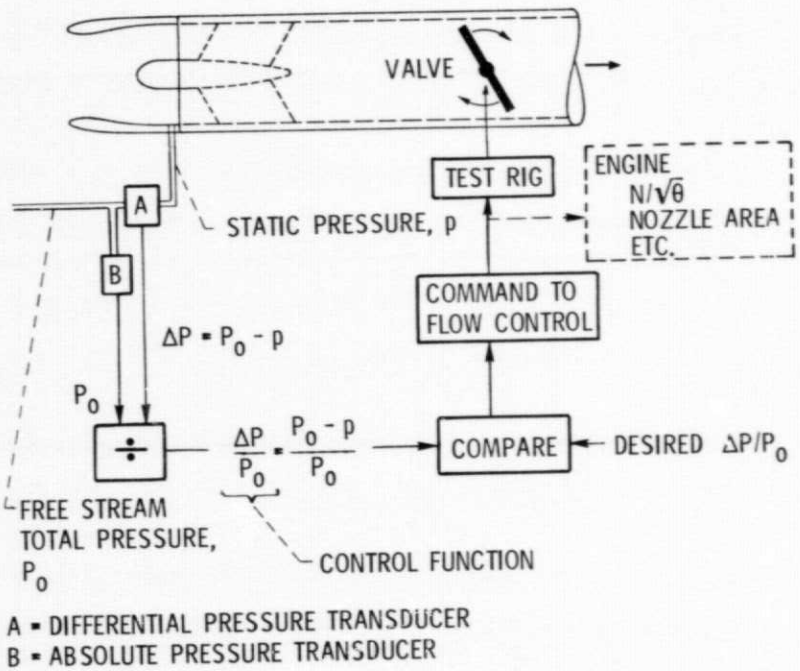

Figure 17. - Schematic of sonic inlet control system tested with fixed geometry sonic inlet.

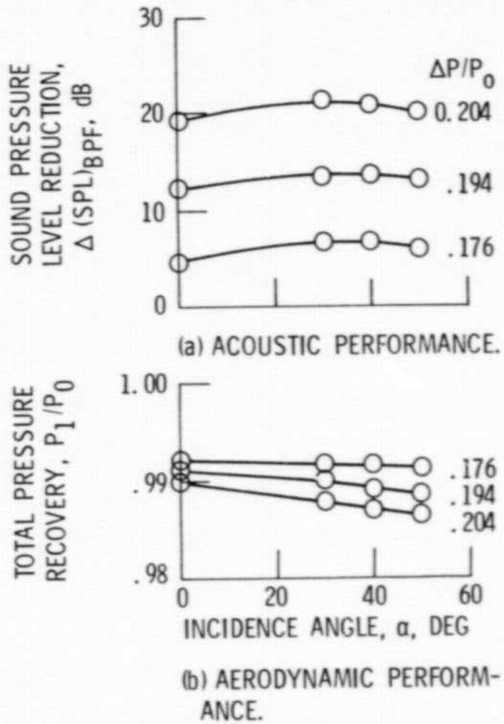

Figure 18. - Sonic inlet aeroacoustic performance obtained with inlet control system. Free stream velocity, V_0, 41 meters per second (80 knots).

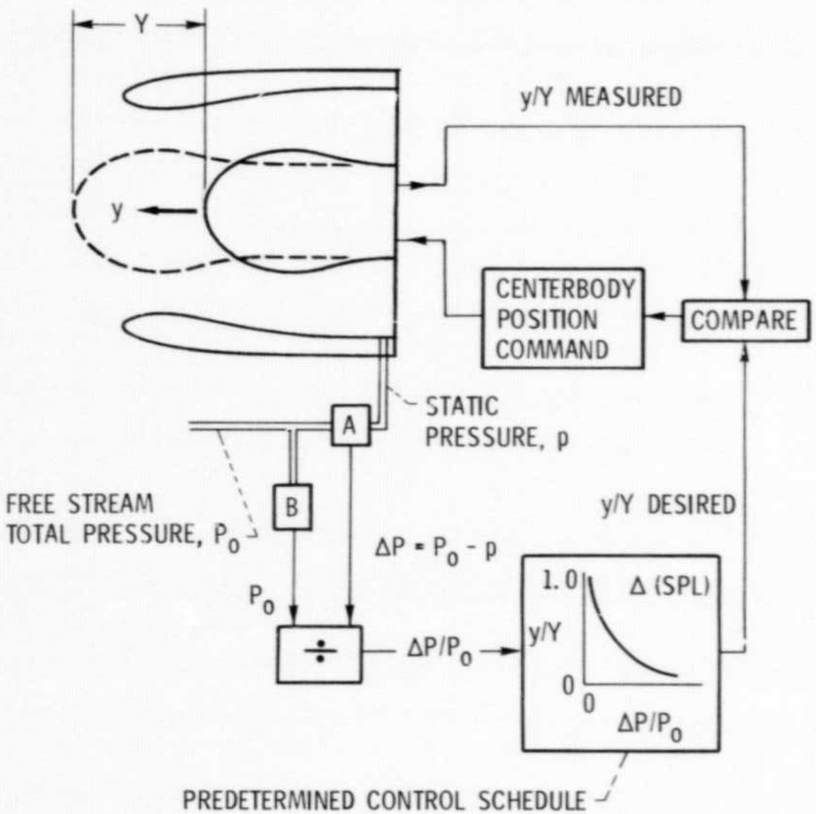

METHOD OF OPERATION:
- INLET AIRFLOW, AND HENCE $\Delta P/P_0$, DICTATED BY ENGINE THRUST SETTING
- CENTERBODY POSITION ADJUSTED USING PREDETERMINED SCHEDULE TO MAINTAIN SPECIFIED Δ (SPL)

Figure 19. - Possible control system for a translating centerbody sonic inlet.

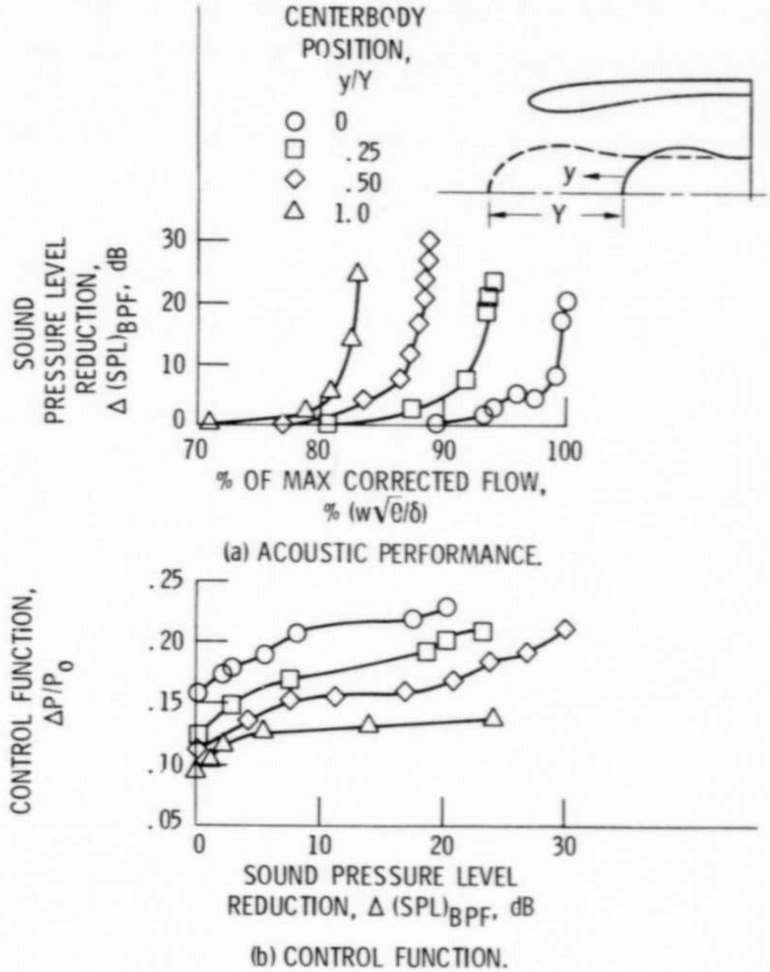

Figure 20. - Translating centerbody sonic inlet acoustic performance and control function. Data obtained at static conditions.

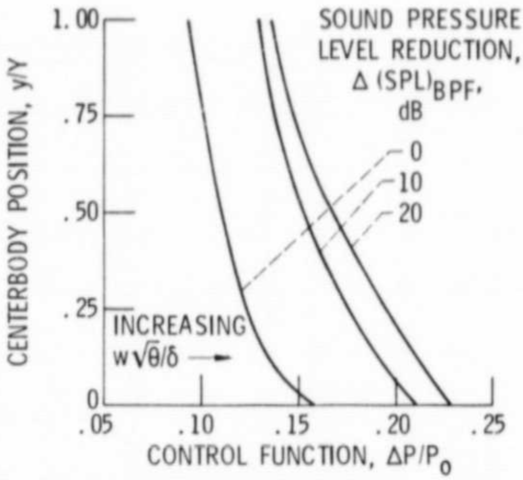

Figure 21. - Translating centerbody sonic inlet control schedule.

E-8422